(1987); D. B. Neal *et al.*, *Electron. Lett.* **22**, 460 (1986); D. Lupo *et al.*, *J. Opt. Soc. Am. B* **5**, 300 (1988).
4. A. Ulman, *Adv. Mater.* **2**, 573 (1990).
5. D. Q. Li *et al.*, *J. Am. Chem. Soc.* **112**, 7389 (1990).
6. T. M. Putvinski *et al.*, *Langmuir* **6**, 1567 (1990).
7. H. Lee, L. J. Kepley, H.-G. Hong, T. E. Mallouk, *J. Am. Chem. Soc.* **110**, 1567 (1988); H. Lee, L. J. Kepley, H.-G. Hong, S. Akhter, T. E. Mallouk, *J. Phys. Chem.* **92**, 2597 (1988).
8. M. B. Dines, P. M. DiGiacomo, *Inorg. Chem.* **20**, 92 (1981); M. B. Dines *et al.*, in *Chemically Modified Surfaces in Catalysis and Electrocatalysis*, J. S. Miller, Ed., no. 192 of *ACS Symposium Series* (American Chemical Society, Washington, DC, 1982), pp. 223–240.
9. H. E. Katz, M. L. Schilling, C. E. D. Chidsey, T. M. Putvinski, R. S. Hutton, *Chem. Mater.* **3**, 699 (1991).
10. Sodium nitrite (0.76 g, 0.011 mol) in 3 ml of H_2O was added dropwise to a suspension of 4-aminophenylphosphonic acid (1.70 g, 0.01 mol) in HCl (4.5 ml) and H_2O (20 ml) cooled to 0°C. As the addition was completed, the solution became homogeneous, and stirring at low temperature was continued for 15 min. Bis(2-hydroxyethyl)aniline (1.8 g, 0.01 mol) was then added, and the solution immediately began turning red, and it continued to darken as the aniline dissolved. After stirring at 0°C for 2 hours, we added solid sodium acetate (1.6 g, 0.02 mol), and the vigorously stirred solution was brought up to room temperature over 1 hour. The mixture was then refrigerated overnight. After being warmed to room temperature, the solution was filtered, and a red-purple solid was collected that was washed with copious amounts of H_2O and dried to give the product, 3.1 g (85% yield). ^1H nuclear magnetic resonance (NMR) (CD_3OD):δ 3.87 (m, 4H, CH_2O, CH_2N), δ 7.15 (d, 2H, ArH), δ 7.90 (m, 6H, ArH). Analysis calculated for $C_{16}H_{20}N_3PO_5$ + 0.5 H_2O: C, 48.98%; H, 5.90%; N, 10.71%; P, 7.89%. Found: C, 49.15; H, 5.52; N, 10.60; P, 7.84.
11. The ellipsometric thicknesses are determined with the refractive index of 1.54 suggested by Mallouk and co-workers (7). The actual value might be somewhat higher because of the presence of the azo dye, but it is difficult to measure in such thin films.
12. All SHG data for the multilayers were referenced to the $\chi^{(2)}_{xxx}$ tensor component of quartz, which was determined by SHG from an antireflection-coated, *y*-cut quartz single crystal with both the fundamental and SHG polarized along the quartz *x*-axis. The angle of incidence was chosen to give the first SHG maximum away from normal incidence [that is, the first Maker fringe maximum (*19*)]. The quartz flat was adequately parallel as judged by the completely destructive interference at the Maker fringe minima. The data were corrected for the polarization response of the spectrometer.
13. The intensity of *p*- and *s*-polarized SHG are, respectively:

$$I_p^{2\omega}(\gamma) = I_{pp\to p}^{2\omega}\cos^4\gamma + I_{ss\to p}^{2\omega}\sin^4\gamma + [I_{pp\to p}^{2\omega} I_{ss\to p}^{2\omega}]^{1/2}\cos\phi\sin^2 2\gamma \quad (4)$$

$$I_s^{2\omega}(\gamma) = I_{sp\to s}^{2\omega}\sin^2 2\gamma \quad (5)$$

where γ is the angle of polarization of the fundamental with respect to the plane of incidence, φ is the phase between the *p*-polarized SHG fields due to the *p*- and *s*-components of the fundamental, and ω is the angular frequency of the light. In transmission, the SHG intensities for the three distinct combinations of polarizations are related to the SHG intensity from quartz by:

$$I_{pp\to p}^{2\omega} = C(\theta)\,|(2d_{xxz} + d_{zxx})\cos^2\theta_f + d_{zzz}\sin^2\theta_f|^2 \quad (6)$$

$$I_{ss\to p}^{2\omega} = C(\theta)\cos^4(\theta_f - \theta)\,|d_{zxx}|^2 \quad (7)$$

$$I_{sp\to s}^{2\omega} = C(\theta)\cos^2(\theta - \theta_s) \times \cos^2(\theta_s - \theta_f)\cos^2(\theta_f - \theta)\,|d_{xxz}|^2 \quad (8)$$

where:

$$C(\theta) = \left[\frac{\pi}{2}\frac{l_f}{l_{quartz}}\right]^2\left[\frac{n_{quartz}}{n_f}\right]^3\frac{I_{quartz}^{2\omega}}{|d_{quartz}|^2} \times [T_p^{a\to f}(\theta)]^2 T_p^{f\to s}(\theta) T_p^{s\to a}(\theta)\frac{\sin^2\theta_f\cos\theta}{\cos^3\theta_f} \quad (9)$$

θ is the angle of incidence, θ_f and θ_s are, respectively, the angles of refraction in the film and the substrate (derived from θ with Snell's law), l_f is the film thickness per layer, l_{quartz} is the coherence length of quartz [20.65 μm (*20*)], n_{quartz} and n_f are the refractive indices of quartz [1.45 (*15*)] and the film [1.54 (*11*)], respectively, d_{quartz} is the nonlinear coefficient of quartz when both the fundamental and second harmonic are polarized along the quartz *x*-axis [0.32 pm/V (*15*)], and $T_p^{i\to j}(\theta)$ is the transmissivity for *p*-polarized light of the interface between phases *i* and *j*, where a, f, and s refer to air, film, and substrate (soda-lime glass with a refractive index of 1.52). All of the *p*-transmissivities are essentially unity for the angle of incidence used here.
14. B. Dick, A. Gieralski, G. Marowsky, G. A. Reider, *Appl. Phys. B* **38**, 107 (1985).
15. S. Singh, in *CRC Handbook of Laser Science and Technology*, M. J. Weber, Ed. (CRC Press, Boca Raton, FL, 1986), pp. 3–220.
16. G. R. Meredith, in *Nonlinear Optical Properties of Organic and Polymeric Materials*, D. J. Williams, Ed. (American Chemical Society, Washington, DC, 1983), pp. 27–56.
17. D. Jungbauer *et al.*, *Appl. Phys. Lett.* **56**, 2610 (1990).
18. W. L. Wilson *et al.*, in preparation.
19. P. D. Maker, R. W. Terhune, M. Nisenoff, C. M. Savage, *Phys. Rev. Lett.* **8**, 21 (1962).
20. J. Jerephagnon and S. K. Kurtz, *Phys. Rev. B* **1**, 1739 (1970).

18 July 1991; accepted 17 September 1991

Tuning High-T_c Superconductors via Multistage Intercalation

X.-D. XIANG, W. A. VAREKA, A. ZETTL,* J. L. CORKILL, T. W. BARBEE III, MARVIN L. COHEN, N. KIJIMA, R. GRONSKY

Multistage intercalation has been used to tune the interaction between adjacent blocks of CuO_2 sheets in the high-T_c (high superconducting transition temperature) superconductor $Bi_2Sr_2CaCu_2O_x$. As revealed by atomic-resolution transmission electron microscopy images, foreign iodine atoms are intercalated into every *n*th BiO bilayer of the host crystal, resulting in structures of stoichiometry $IBi_{2n}Sr_{2n}Ca_nCu_{2n}O_x$ with stage index *n* up to 4. An expansion of 3.6 angstroms for each intercalated BiO bilayer decouples the CuO_2 sheets in adjacent blocks. A comparison of the superconducting transition temperatures of the pristine host material and intercalated compounds of different stages suggests that the coupling between each pair of adjacent blocks contributes ~5 K to T_c in $Bi_2Sr_2CaCu_2O_x$.

ALTHOUGH IT IS GENERALLY BELIEVED that the critical structural units in the highest T_c superconductors are the CuO_2 planes, the significance of coupling between the planes is poorly understood. It was recently demonstrated that, like many other two-dimensional materials, Bi-based high-T_c superconducting oxides can be intercalated with foreign species (*1*). For stage-1 iodine-intercalated $Bi_2Sr_2CaCu_2O_x$, guest iodine atoms are introduced between every pair of weakly bonded BiO bilayers, thus affecting the coupling between identical host blocks containing the double CuO_2 planes. In some intercalation compounds, higher stage structures are possible; a stage-*n* structure has *n* identical host layers or blocks sandwiched between each pair of intercalant layers. High-stage single-phase graphite intercalation compounds can be synthesized with *n* as high as 8 (*2*), but in other layered compounds it is difficult to achieve single-phase intercalation with $n > 1$. The possibility of using intercalants to vary the strength of interlayer interactions and possibly modify microscopic charge transfer makes the intercalation of high-T_c compounds attractive. Systematic investigation of the superconductivity mechanism and its relation to crystal structure is possible if different intercalants can be incorporated and higher stage compounds can be generated.

We here examine interblock interactions in the high-T_c superconductor $Bi_2Sr_2CaCu_2O_x$ by using multistage iodine intercalation to "tune" the coupling between adjacent CuO_2-containing blocks. Atomic resolution real-space transmission electron microscopy (TEM) images identify stage structures with $n \leq 4$. Correlations between the crystal structure and T_c allow us to determine the contributions to T_c of interblock CuO_2 plane interactions and to evaluate various models for the superconductivity mechanism.

In the intercalation of pristine Bi_2Sr_2Ca-

X.-D. Xiang, W. A. Vareka, A. Zettl, J. L. Corkill, T. W. Barbee III, M. L. Cohen, Department of Physics, University of California at Berkeley, and Materials Sciences Division, Lawrence Berkeley Laboratory, Berkeley, CA 94720.
N. Kijima and R. Gronsky, Department of Materials Science and Mineral Engineering, University of California, and National Center for Electron Microscopy, Materials Sciences Division, Lawrence Berkeley Laboratory, Berkeley, CA 94720.

*To whom correspondence should be addressed.

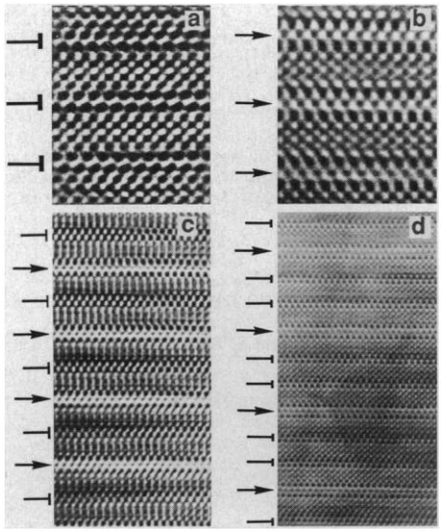

Fig. 1. Processed TEM images of the crystal structures of the (**a**) pristine, (**b**) stage-1, (**c**) stage-2, and (**d**) stage-3 phases of iodine-intercalated $Bi_2Sr_2CaCu_2O_x$. Bars identify the pristine-like BiO bilayers, and arrows identify the iodine-intercalated BiO bilayers.

Cu_2O_x crystals we used a gas diffusion technique similar to that described elsewhere (*1*). For high-stage intercalation, iodine and $Bi_2Sr_2CaCu_2O_x$ crystals were placed in evacuated cells with a common connection for vapor transport. The iodine cell was held at 150°C and the sample cell at between 300° and 350°C, for up to 2 weeks. Intercalated crystal structures were characterized by x-ray diffraction and by TEM. In general, intercalation resulted in a complete disappearance of the pristine phase. As with stage-1 materials, nearly phase-pure stage-2 materials could be produced. Stage-3 and stage-4 structures were obtained only as minority phases.

Figure 1, a through d, shows real-space TEM images, respectively, for pristine $Bi_2Sr_2CaCu_2O_x$ and stage-1, stage-2, and stage-3 iodine-intercalated crystals, all viewed along the [110] direction. In each case, pristine-like BiO bilayers are identified by bars and iodine-intercalated BiO bilayers by arrows. The image in Fig. 1a agrees with the established crystal structure of pristine $Bi_2Sr_2CaCu_2O_x$. For the stage-1 material (Fig. 1b), iodine is intercalated into every BiO bilayer; for the stage-2 material (Fig. 1c), iodine is intercalated into every other BiO bilayer; for the stage-3 material (Fig. 1d), iodine is intercalated into every third BiO bilayer. The resulting intercalated stage structures have stoichiometry $IBi_{2n}Sr_{2n}Ca_{2n}Cu_{2n}O_x$, where n is the stage index. Structures with $n \leq 4$ have been identified in TEM images. In all cases, the iodine intercalation is epitaxial (the iodine is located between oxygens of the BiO layers) and results in two major structural changes. First, it expands each intercalated BiO bilayer by 3.6 Å along the c axis. Second, it changes the staggered Bi atom stacking sequence (between adjacent BiO bilayers) to a commonly registered stacking sequence. For example, the stacking sequence AB . . .BA. . .AB relevant to pristine $Bi_2Sr_2CaCu_2O_x$ changes in the stage-2 compound to AB. . .B/B. . .BA. . .A/A. . .AB. A and B represent BiO layers shifted by 1/2 a with respect to each other, the dotted lines represent the other elements inside the block, and the slash represents the iodine intercalant.

The ability to produce largely homogeneous stage-1 and stage-2 compounds of $IBi_{2n}Sr_{2n}Ca_nCu_{2n}O_x$ allows a direct comparison between structural and superconducting properties. Figure 2 shows the magnetic susceptibility, χ_{ac}, as a function of temperature for pristine $Bi_2Sr_2CaCu_2O_x$, stage-1 $IBi_2Sr_2CaCu_2O_x$, and stage-2 $IBi_4Sr_4Ca_2Cu_4O_x$. Well-defined transitions to the superconducting state are visible in each case. Consistent with previous studies, T_c for stage-1 iodine-intercalated $IBi_2Sr_2CaCu_2O_x$ is 80 K, corresponding to a ~10 K depression in T_c compared to the pristine host material. T_c for stage-2 $IBi_4Sr_4Ca_2Cu_4O_x$ is 85 K, corresponding to a ~5 K depression in T_c.

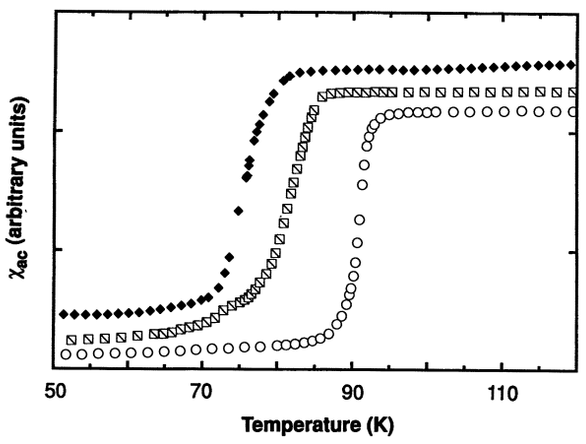

Fig. 2. Plot of the ac magnetic susceptibility, χ_{ac}, of pristine (○), stage-1 (◆), and stage-2 (▨) phases versus temperature.

It is unlikely that the shift in T_c is due to charge transfer between the iodine and host material. The iodine is only weakly bonded to the BiO layers, and the distance between the intercalated layers and the CuO_2 layers is large. Transport measurements (*3*) on the stage-1 material have confirmed that the normal state behavior of the CuO_2 planes remains unchanged by the intercalation. The shift in T_c for different intercalation stage structures can therefore be assumed to be a consequence of changes in the interblock coupling (*4, 5*). The dominant effect of intercalation is to reduce interblock coupling, which results from an increase in the distance between the CuO_2-containing blocks. Stage-1 intercalation reduces the adjacent block coupling in both directions along the c axis, whereas stage-2 intercalation preserves the original coupling in one direction for each block. Because ΔT_c for the stage-1 material is -10 K while ΔT_c for the stage-2 material is only -5 K, empirically it appears as if next-block coupling contributes about 5 K to T_c for each neighboring block of pristine $Bi_2Sr_2CaCu_2O_x$.

Our results suggest that, independent of the specific pairing mechanism, interblock coupling should be incorporated into any realistic model of high-T_c superconductivity. Here we examine two prototypical layering models; both are capable of accounting for the behavior of T_c upon multistage intercalation. No specific microscopic mechanism is assumed, and the parameters in each model are determined here phenomenologically.

The simplest layer-coupling model is one in which T_c varies linearly with the interplane coupling. Each CuO_2 plane is coupled to its neighbors in the c direction, but intraplane coupling is neglected. Wheatley, Hsu, and Anderson (*6*) used this type of model to discuss superconductivity due to spinon-holon scattering. Despite inconsistencies in the spinon-holon theory as a whole revealed by transport measurements (*3*), the layering model used by Wheatley *et al.* is non-mechanism–specific. Here we apply the layering scheme to the present experiment to discuss the effects of intercalation and exhibit the merits of this approach.

In the linear layering model, the superconducting amplitude in plane i, η_i, depends on η_{i+1} and η_{i-1} and the couplings between the planes, $\lambda_{i,i+1}$ and $\lambda_{i,i-1}$. For $Bi_2Sr_2CaCu_2O_x$, there are two different couplings, λ_0 and λ_1, for nearest and next nearest planes, respectively. The nearest planes are within a block, whereas the next nearest planes are in adjacent blocks. Because all the CuO_2 planes are equivalent, all the η's are equal and the eigenvalue equation for T_c,

$$(\lambda_0 + \lambda_1)\eta = T_c\eta \quad (1)$$

yields T_c(pristine) = $\lambda_0 + \lambda_1$.

For stage-1 $IBi_2Sr_2CaCu_2O_x$, the model is the same but with λ_1 replaced by λ_1' because the next nearest plane coupling is assumed to be grossly affected by the intercalation. The predicted stage-1 T_c is then $\lambda_0 + \lambda_1'$.

For stage-2 $IBi_4Sr_4Ca_2Cu_4O_x$, the CuO_2 planes are no longer equivalent; there are planes (a) coupled by λ_0 and λ_1 and planes (b) coupled by λ_0 and λ_1'. The eigenvalue equation for T_c is then

$$T_c\begin{pmatrix}\eta_a\\ \eta_b\end{pmatrix} = \begin{bmatrix}\lambda_1 & \lambda_0\\ \lambda_0 & \lambda_1'\end{bmatrix}\begin{pmatrix}\eta_a\\ \eta_b\end{pmatrix} \quad (2)$$

If we assume that intercalation completely destroys the next nearest plane coupling, then $\lambda_1' \to 0$, and the measured T_c(stage-1) yields λ_0 = 80 K. With T_c(stage-2) = 85 K, λ_0 = 80 K, and λ_1' = 0 K, we find λ_1 = 9.7 K. This is consistent with the results for the pristine material, where T_c is typically 90 K [= ($\lambda_0 + \lambda_1$)].

It is possible to use the above analysis to predict the T_c's for higher stage compounds. If λ_0 = 80 K, λ_1 = 10 K, and λ_1' = 0 K, the predicted T_c's for stages 3, 4, 5, and 6 are 87, 88, 89, and 89 K, respectively. Although we have demonstrated that stage-3 and stage-4 structures exist for iodine-intercalated $Bi_2Sr_2CaCu_2O_x$, we have not been able to reliably determine the T_c's for these minority phases.

A second approach incorporates interplane interactions into a Bardeen-Cooper-Schrieffer (BCS)–like framework. Such a model has been advanced by Ihm and Yu (7), although they neglected interblock coupling. Because our experiments indicate that this coupling cannot be neglected, we incorporate such a coupling into a phenomenological model (which is essentially an extension of the original work of Ihm and Yu).

Solving the BCS-like gap equations, assuming a constant density of states per CuO_2 plane (even after intercalation), one obtains

$$F(\text{pristine}) = \left(\frac{1}{\lambda_a + \lambda_{er} + \lambda_n}\right) \quad (3)$$

$$F(\text{stage-1}) = \left(\frac{1}{\lambda_a + \lambda_{er}}\right) \quad (4)$$

$$F(\text{stage-2}) \approx \left(\frac{1}{\lambda_a + \lambda_{er} + \frac{\lambda_n}{2}}\right) \quad (5)$$

$$F(\text{Bi-2223}) = \left(\frac{1}{\lambda_a + \sqrt{2}\lambda_{er} + \lambda_n}\right) \quad (6)$$

where $F(\Delta_\epsilon) = \int_0^{\hbar\omega} \tanh[(\epsilon^2 + \Delta_\epsilon^2)^{1/2}/2kT]/(\epsilon^2 + \Delta_\epsilon^2)^{1/2} d\epsilon$ is the gap function ($\hbar$ is Planck's constant divided by 2π, ω is frequency, ϵ is energy, k is Bolzmann's constant; $\lambda_a(\lambda_{er})$ is $N(\epsilon_f)V_a$ [$N(\epsilon_f)V_{er}$], the intraplane and nearest CuO_2 plane couplings (7); and λ_n is $N(\epsilon_f)V_n$, the next block coupling [$N(\epsilon_f)$ is the density of states at the Fermi level, and V is the strength of the interaction].

In this model, F determines T_c through $kT_c \cong 1.14\ \hbar\omega \exp(-F)$. If we fit the coupling parameters λ_a, λ_{er}, and λ_n for $\hbar\omega$ = 0.1 eV to the experimentally determined T_c's of pristine $Bi_2Sr_2Ca_2Cu_3O_x$ (Bi-2223) (T_c = 110 K) and the pristine and stage-1 $IBi_2Sr_2CaCu_2O_x$ compounds, we obtain λ_a = 0.2840, λ_{er} = 0.0725, and λ_n = 0.0156. Although λ_n is small (~5% of λ_a), it is over 20% of the size of λ_{er} and not negligible. With these parameters, this model predicts the stage-2 T_c to be 84.9 K, in excellent agreement with the experimentally determined T_c = 85 K. Hence, with interblock coupling included, a BCS-like model accounts well for the intercalation-induced shift in T_c for the stage-2 material. The model can also be extended to predict the T_c's of higher stage compounds, although the dependence of F on the coupling is much more complex than for lower stages.

In conclusion, we have shown that high-stage iodine intercalation of $Bi_2Sr_2CaCu_2O_x$ is possible. The shifts in T_c of the intercalated materials demonstrate that interblock coupling is an important ingredient in describing high-T_c copper oxides. In $Bi_2Sr_2CaCu_2O_x$, coupling between each pair of adjacent CuO_2-containing blocks contributes ~5 K to T_c.

REFERENCES AND NOTES

1. X.-D. Xiang *et al.*, *Nature* **348**, 145 (1990); X.-D. Xiang *et al.*, *Phys. Rev. B* **43**, 11496 (1991).
2. P. Levy, *Intercalated Layered Materials* (Reidel, Dordrecht, 1979).
3. X.-D. Xiang *et al.*, unpublished data.
4. D. H. Lowndes, D. P. Norton, J. D. Budai, *Phys. Rev. Lett.* **65**, 1160 (1990).
5. J.-M. Triscone, M. G. Karkut, L. Antognalla, A. Brunner, O. Fisher, *ibid.* **63**, 1016 (1989).
6. J. M. Wheatley, T. C. Hsu, P. W. Anderson, *Nature* **333**, 121 (1988).
7. J. Ihm and B. D. Yu, *Phys. Rev. B* **39**, 4760 (1989).

8. This work was supported by the director, Office of Energy Research, Office of Basic Energy Sciences, Materials Sciences Division of the U.S. Department of Energy under contract DE-AC03-76SF00098. J.L.C., T.W.B., and M.L.C. were also supported by National Science Foundation grant DMR88-18404. J.L.C. acknowledges support from an AT&T Ph.D. fellowship. M.L.C. acknowledges support from the J.S. Guggenheim Foundation.

10 September 1991; accepted 4 October 1991

Phase Transformations in Carbon Fullerenes at High Shock Pressures

C. S. YOO AND W. J. NELLIS

C_{60} powders were shock-compressed quasi-isentropically and quenched from pressures in the range 10 to 110 GPa (0.1 to 1.1 Mbar). Recovered specimens were analyzed by Raman spectroscopy and optical microscopy. C_{60} fullerenes are stable into the 13- to 17-GPa pressure range. The onset of a fast (~0.5 μs) reconstructive transformation to graphite occurs near 17 GPa. The graphite recovered from 27 GPa and about 600°C is relatively well ordered with crystal planar domain size of about 100 Å. Above 50 GPa a continuous transformation to an amorphous state is observed in recovered specimens. The fast transformation to graphite is proposed to occur by π-electron rehybridization which initiates breakup of the ball structure and formation of the graphite structure at high density.

THE FULLERENE MOLECULES (C_{60}) have a high-symmetry truncated icosahedral structure (*1*), which is very stable, despite the hollow cage with large strains in π-bonds and inherent structural "defects," the five-membered rings (*2*). The pseudospherical structure of C_{60} with diameter d_a = 7.1 Å is stable to a pressure of at least 20 GPa (200 kbar) at ambient temperature (*3*) and theoretically to 1800 K at ambient pressure (*4*). Introducing metal atoms between C_{60} balls induces little structural distortion (*5*). The exceptional stability of C_{60} is a central issue for developing new materials such as lubricants, ultrastrong fibers, hard materials, and high-temperature superconductors (*6*). For this reason it is important to determine the stability range of fullerenes at high pressures and temperatures.

C_{60} crystals, fullerites, order in a face-centered cubic (fcc) phase (*7*) with an extraordinarily weak van der Waals interaction between molecules, which causes a large compressibility at low static pressures (*3*).

Physics Department, H Division and Institute of Geophysics and Planetary Physics, Lawrence Livermore National Laboratory, University of California, Livermore, CA 94550.